

Modulation response of a long-cavity, gain-levered quantum-dot semiconductor laser

Michael Pochet,^{1,*} Nicholas G. Usechak,² John Schmidt,¹ and Luke F. Lester³

¹Department of Electrical and Computer Engineering, US Air Force Institute of Technology, Wright-Patterson Air Force Base, Ohio 45433, USA

²Sensors Directorate, US Air Force Research Laboratory, Wright-Patterson Air Force Base, Ohio 45433, USA

³Bradley Department of Electrical and Computer Engineering, Virginia Polytechnic Institute and State University, Blacksburg, Virginia 24061, USA

*michael.pochet@afit.edu

Abstract: The gain-lever effect enhances the modulation efficiency of a semiconductor laser when compared to modulating the entire laser. This technique is investigated in a long-cavity multi-section quantum-dot laser where the length of the modulation section is varied to achieve 14:2, 15:1 and 0:16 gain-to-modulation section ratios. In this work, the gain-levered modulation configuration resulted in an increase in modulation efficiency by as much as 16 dB. This investigation also found that the 3-dB modulation bandwidth and modulation efficiency are dependent on the modulation section length of the device, indicating the existence of an optimal gain-to-modulation section ratio. The long cavity length of the multi-section laser yielded a distinctive case where characteristics of both the gain-lever effect and spatial effects are observed in the modulation response. Here, spatial effects within the cavity dominated the small-signal modulation response close to and above the cavity's free-spectral range frequency, whereas the gain-lever effect influenced the modulation response throughout the entirety of the response.

©2014 Optical Society of America

OCIS codes: (060.4080) Modulation; (230.5590) Quantum-well, -wire and -dot devices; (140.5960) Semiconductor lasers.

References and links

1. K. J. Vahala, M. A. Newkirk, and T. R. Chen, "The optical gain lever: A novel gain mechanism in the direct modulation of quantum well semiconductor lasers," *Appl. Phys. Lett.* **54**(25), 2506–2508 (1989).
2. Y. Li, N. A. Naderi, V. Kovanis, and L. F. Lester, "Enhancing the 3-dB bandwidth via the gain-lever effect in quantum-dot lasers," *IEEE Photon. J.* **2**(3), 321–329 (2010).
3. T. B. Simpson, J. M. Liu, and A. Gavrielides, "Bandwidth enhancement and broad-band noise-reduction in injection-locked semiconductor-lasers," *IEEE Photon. Technol. Lett.* **7**(7), 709–711 (1995).
4. A. Murakami, K. Kawashima, and K. Atsuki, "Cavity resonance shift and bandwidth enhancement in semiconductor lasers with strong light injection," *IEEE J. Quantum Electron.* **39**(10), 1196–1204 (2003).
5. M. Radziunas, A. Glitzky, U. Bandelow, M. Wolfrum, U. Troppenz, J. Kreissl, and W. Rehbein, "Improving the modulation bandwidth in semiconductor lasers by passive feedback," *IEEE J. Sel. Top. Quantum Electron.* **13**(1), 136–142 (2007).
6. F. Grillot, C. Wang, N. A. Naderi, and J. Evan, "Modulation properties of self-injected quantum-dot semiconductor diode lasers," *IEEE J. Sel. Top. Quantum Electron.* **19**(4), 1900812 (2013).
7. M. Asada, Y. Mitamoto, and Y. Suematsu, "Gain and the threshold of three-dimensional quantum-box lasers," *IEEE J. Quantum Electron.* **22**(9), 1915–1921 (1986).
8. L. F. Lester, S. D. Offsey, B. K. Ridley, W. J. Schaff, B. A. Foreman, and L. F. Eastman, "Comparison of the theoretical and experimental differential gain in strained layer InGaAs/GaAs quantum well lasers," *Appl. Phys. Lett.* **59**(10), 1162–1164 (1991).
9. M. G. Thompson, A. R. Rae, M. Xia, R. V. Penty, and I. H. White, "InGaAs quantum-dot mode-locked laser diodes," *IEEE J. Sel. Top. Quantum Electron.* **15**(3), 661–672 (2009).
10. C. R. Doerr, "Direct modulation of long-cavity semiconductor lasers," *J. Lightwave Technol.* **14**(9), 2052–2061 (1996).
11. N. G. Usechak, M. Grupen, N. Naderi, Y. Li, L. F. Lester, and V. Kovanis, "Modulation effects in multi-section semiconductor lasers," *Proc. SPIE* **7933**, 793311 (2011).

12. L. A. Coldren and S. W. Corzine, *Diode Lasers and Photonic Integrated Circuits* (John Wiley & Sons, Inc., 1995), pp. 204–207.
 13. Y. Li, N. A. Naderi, Y.-C. Xin, C. Dziak, and L. F. Lester, “Multi-section gain-lever quantum dot lasers,” *Proc. SPIE* **6468**, 646819 (2007).
 14. N. Naderi, M. Pochet, F. Grillot, N. Terry, V. Kovanis, and L. F. Lester, “Modeling the injection-locked behavior of a quantum dash semiconductor laser,” *IEEE J. Sel. Top. Quantum Electron.* **15**(3), 563–571 (2009).
 15. L. A. Glasser, “A linearized theory for the diode laser in an external cavity,” *IEEE J. Quantum Electron.* **16**(5), 525–531 (1980).
-

1. Introduction

This paper investigates the impact of different gain-lever configurations on the frequency response of a long-cavity multi-section quantum-dot semiconductor laser. The gain-lever effect is a method designed to enhance the modulation efficiency of directly modulated semiconductor lasers [1]. Under the gain-lever effect a two-section laser is biased asymmetrically to facilitate operation at two different points on the gain profile of the laser’s active region. As a consequence of the relationship between differential gain and carrier density, cavity photons may be more efficiently modulated in a section subject to a lower biasing current [1]. While improving the modulation efficiency, the gain-lever effect is also observed to enhance the 3-dB modulation bandwidth [2]; such improvements achieved through the alteration of a laser’s electrical biasing conditions are highly attractive, given that various other means of improving a laser’s modulation characteristics involve external light sources (optical injection-locking) [3, 4] or external feedback control mechanisms [5, 6].

The gain-levering of *quantum-dot* lasers is of particular interest due to their characteristically large differential gain under weak bias conditions (low carrier density), and saturated gain profile (negligible differential gain) under high current densities [7–9]. This suppressed differential gain at high carrier densities is pronounced in quantum-dot lasers when compared to the gain profile of both quantum-well and bulk gain region devices [7, 8]. While previous studies of the gain-lever effect in quantum-dot lasers have utilized 4:1 gain-to-modulation section ratios in short-cavity lasers (< 1 mm) [2], this work investigates an extreme gain-lever case, where the gain-to-modulation section ratio is 15:1 in a long-cavity laser (> 8 mm). These unique experimental results of representative extreme asymmetric bias cases (15:1 and 14:2) highlight the limit to the gain-to-modulation section ratio discussed numerically in [2] and compared with the single-section modulation response (0:16).

Reconfigurability of the biasing architecture was achieved by the addition and/or removal of wire bonds connecting the electrically isolated sections of the laser. By studying a 8.3-mm long laser, spatial effects within the laser’s cavity play a role in the modulation response and were also experimentally studied [10, 11]. Although not the focus of this work, the observed spatial effects, noticeable in the small-signal modulation transfer response at the free-spectral range frequency of the device (and subsequent higher order harmonics), indicate shortcomings of the widely accepted analytic modulation transfer function derived from the spatially independent rate equations describing the photon and carrier density within the optical cavity [11, 12]. The combined effects of both the cavity’s spatial effects and the gain-lever effect achieved by asymmetrically biasing the laser yields a case where the 3-dB small-signal modulation bandwidth can extend beyond the laser’s free-spectral range.

2. Methodology and experimental setup

The layout of the long-cavity multi-section quantum-dot laser is depicted in Fig. 1, where wire bonds were used to connect a segmented probe card to the semiconductor laser. A Cascade Microsystems high-speed probe (40-GHz bandwidth) was used to apply both DC bias current and the microwave frequency to the section(s) being modulated. The remaining gain sections of the semiconductor laser were biased using DC probes. The output of the laser was coupled into a lensed fiber aligned with the laser’s active region using a piezoelectric-controlled stage while the temperature of the mounted laser was held constant at a 25 °C. An

Agilent N4373C Lightwave Component Analyzer was used to measure the S_{21} modulation responses shown in Figs. 4-7. The overall experimental configuration is given in Fig. 2.

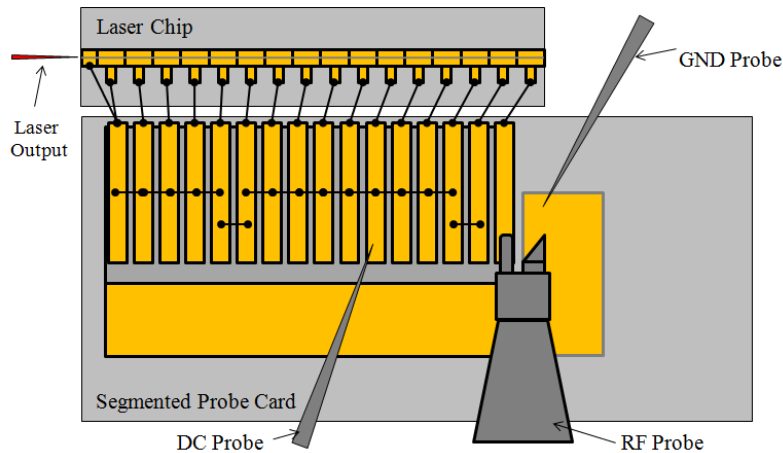


Fig. 1. Layout of the multi-section laser. As shown, one 0.5-mm section of the laser is modulated using the ground-signal microwave probe. The remaining 15 sections are DC biased to yield a 15:1 gain-to-modulation section ratio.

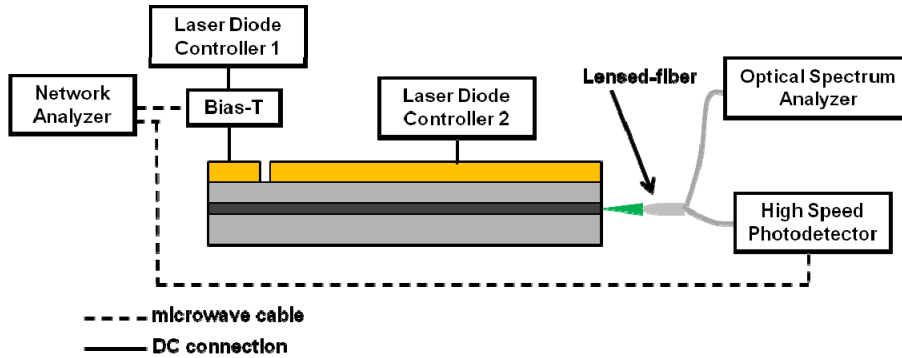


Fig. 2. Experimental setup to measure the modulation transfer response of the multi-section laser. The bias-T, high-speed photodetector, and microwave cables had a bandwidth of at least 26.5 GHz.

The 8.3-mm long laser under test was comprised of 16 electrically-isolated 0.5-mm long sections (via ion implantation) and one 0.3-mm section at the output facet (see Fig. 1). The single 0.3-mm section was shorted to the adjacent 0.5-mm section, yielding a total of 16 sections; the laser is henceforth referred to as a 16-section device. While the single 0.3-mm section results in the experimental realization of 15.6:1 and 14.6:2 gain-to-modulation section length ratios, integer simplifications of 15:1 and 14:2 ratios are used throughout the manuscript to simplify nomenclature. The region which accomplishes the electrical isolation between each p -contact metallization section is pictured in the scanning electron microscope image in Fig. 3. The isolation region between each of the 16 sections is $\sim 9 \mu\text{m}$ in length, resulting in $\sim 150 \mu\text{m}$ of non-biased cavity length. The laser facets were coated with 5/95 low-reflectivity/high-reflectivity coatings. The operating wavelength was 1234 nm and a threshold current of 46 mA (138.6 A/cm^2) was measured. A detailed description of the quantum-dot material used for the laser can be found in [8]. The material properties and cavity length resulted in a free-spectral range $\sim 5 \text{ GHz}$, well below the $80 + \text{ GHz}$ range common for ≤ 0.5 -mm long cavity semiconductor lasers.

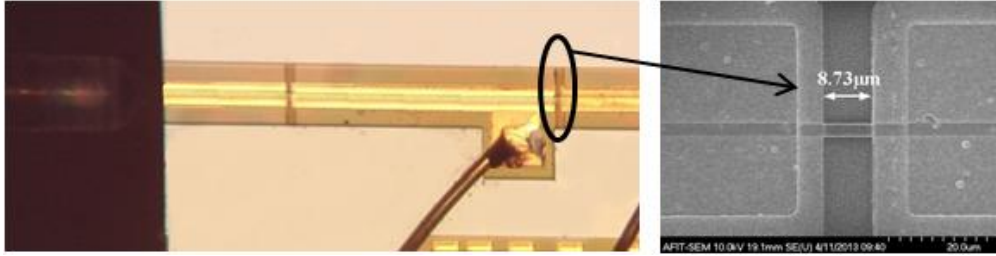


Fig. 3. Optical (left) and scanning electron microscope (SEM) (right) images of the multi-section laser. The SEM image highlights the width of the gap between the ohmic contacts.

3. Results

The reconfigurable nature of the multi-section device facilitated the testing of extreme gain-to-modulation section cases in an attempt to determine a relationship between modulation section length and enhancement of both the modulation efficiency and modulation bandwidth. The modulation response for three cases: single-section (0:16), 15:1, and 14:2, are shown in Fig. 4. The single-section case describes a configuration where all 16 sections of the laser are shorted together and therefore is expected to behave as a convention ‘single-section’ laser. The 15:1 and 14:2 configurations indicate cases where two electrically isolated electrical connections are made to the laser in the ratio described. In Fig. 4, a DC bias of 200 mA is applied to the single-section configuration; for the 14:2 and 15:1 two-section gain-lever effect cases, the modulation section was biased at the threshold current level and the gain section was biased to yield an output power equal to that of the single-section case at 200 mA. The 14:2 configuration has a 3-dB bandwidth of 2.7 GHz, while the 15:1 and single-section configurations both have bandwidths of ~ 2.2 GHz. The modulation response data for each configuration was normalized to 0 dB in order to make accurate comparisons between each modulation response (S_{21}) curve.

The prominent peak at ~ 5 GHz coincides with the free-spectral range of the laser cavity. For the single-section case, the resonant enhancement at the free-spectral range is not predicted by the commonly accepted analytic modulation response function for a single-section laser [12], is found to disappear in computer simulations which include spatial effects [11], and should not be observed experimentally. Nevertheless, our data includes this feature which can be explained as a result of e.g. the 16 electrical isolation sections (Figs. 1 and 3), the non-uniform biasing in the cavity due to the multi-section nature, and/or the atypically long length of the cavity.

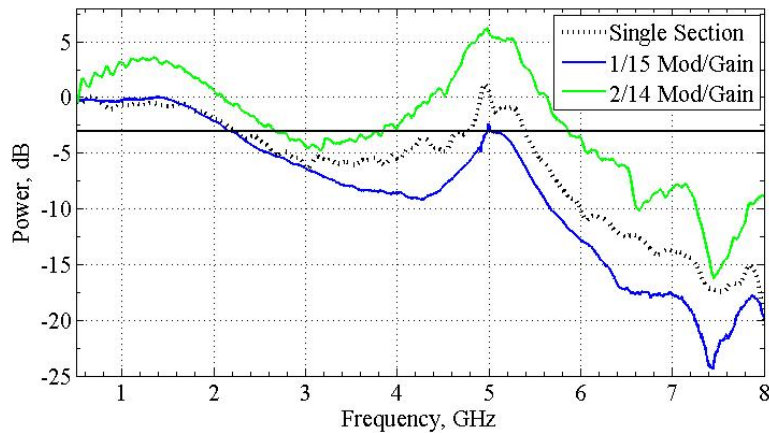


Fig. 4. The gain-lever effect on the 3-dB modulation (S_{21}) bandwidth. A bias current of 200 mA was applied to the single-section case. For the 14:2 and 15:1 cases, the modulation section was biased at the threshold current level and the gain section was biased to yield an output power equal to the single-section case.

One observation from Fig. 4 is that the modulation of only one 0.5-mm section (15:1 ratio case) possessed a 3-dB bandwidth less than that of the 14:2 ratio case. There are two possible explanations for this behavior. One is that the 0.5-mm section is too short to provide enough modulation strength to affect the entirety of the laser cavity. Another feasible explanation is that the RF signal power is saturating the small section even though the DC bias is just above the threshold current density. Regardless of the cause, it suggests that there is an optimal modulation section length for the gain-lever effect at a specific current. Indeed, the modulation of a substantially short, weakly biased section will eventually result in a negligible change in photon density as a result of saturation effects. On the other hand, if the entire device is modulated, the standard two-pole response is found and a less-than-optimal differential gain is realized limiting the modulation efficiency of the device. It also implies that the approximations used in deriving the analytic modulation response of a gain-levered laser do not hold for this long-cavity, multi-section quantum-dot device [2, 13]. A corresponding response is given in Fig. 5, where the DC bias current applied to the single-section case is 100 mA. The experimental results of both Figs. 4 and 5 show that the modulation response is influenced by the gain-lever effect throughout the entirety of the modulation response. Moreover, the 15:1 gain-lever effect case does not result in an improvement to the 3-dB modulation bandwidth when compared to the single-section case.

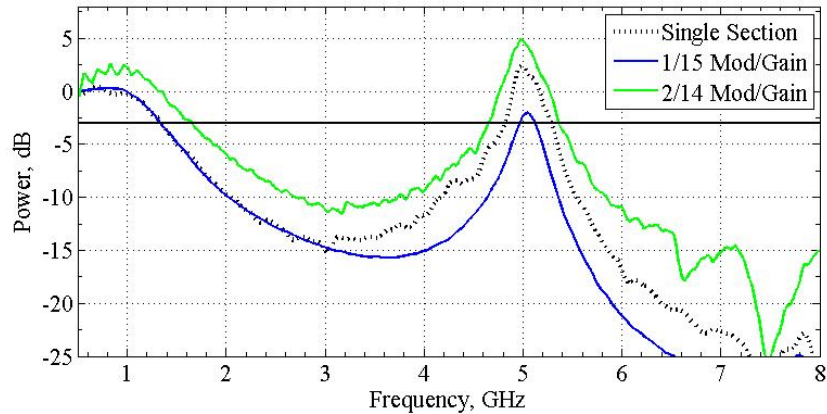


Fig. 5. The gain-lever effect on the 3-dB modulation (S_{21}) bandwidth. A bias current of 100 mA was applied to the single-section case. For the 14:2 and 15:1 cases, the modulation section was biased at the threshold current level and the gain section was biased to yield an output power equal to the single-section case.

Increasing the bias current in the gain section, while maintaining the DC bias applied to the modulation section at the threshold current level, resulted in a case where the dip in the modulation response between the resonance frequency and the free-spectral range of the device was significantly reduced. The reduction of this dip yielded a case where the 3-dB modulation bandwidth extended *beyond* the enhanced resonance at the free-spectral range frequency, giving a 3-dB modulation bandwidth of 6.3 GHz; this value is $\sim 2X$ that of the single-section case. This case, observed using a 14:2 gain-to-modulation section ratio, is given in Fig. 6.

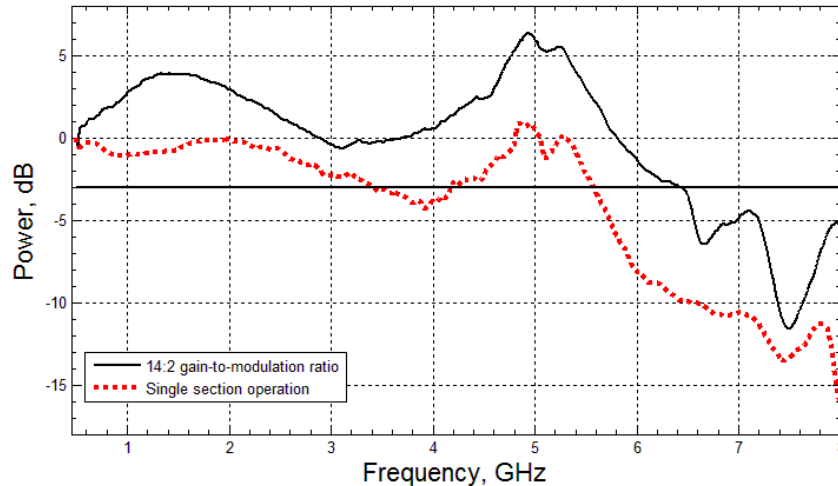


Fig. 6. Combined gain-lever effect and spatial effects extending the 3-dB modulation (S_{21}) bandwidth beyond the laser's free-spectral range. A 14:2 gain-to-modulation ratio was implemented, where the modulation section was biased at the threshold level and the current applied to the gain section was adjusted to yield an output power equivalent to the 300-mA single-section case. The 300mA single-section case is appended for comparison purposes.

Specific focus was also placed on the modulation efficiency enhancement achievable as the carrier density in the modulation section was varied. Measurements were performed utilizing the 15:1 gain-to-modulation section configuration, where the gain-to-modulation

section bias current ratio was varied. Three representative results are plotted in Fig. 7, where an appreciable increase in the modulation efficiency of the modulation response is shown as the DC conditions are varied. The least responsive (lowest modulation efficiency) case was observed under uniform bias conditions; this case describes all 16 sections of the device being biased at the same current density, 500 A/cm², while only one section was RF modulated. This modulation efficiency improvement result agrees with theoretical predictions, given the saturated gain at this bias condition [2, 7]. For each case where the bias in the modulation section was reduced, the gain section's bias current was increased to maintain a constant output power. It is noted that with further reduction of the bias current in the modulation section (below threshold), the overall amplitude of the modulation response drops substantially. Overall, a 16-dB improvement to the modulation efficiency (at 0.4-GHz) was observed.

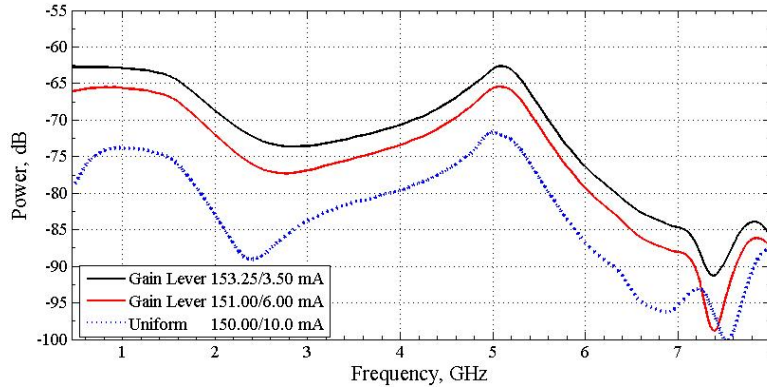


Fig. 7. 15:1 gain-to-modulation section architecture; varied asymmetric bias conditions. The output power was held constant at 3.2 mW for all bias configurations. A 16-dB improvement to the modulation efficiency is reported.

Characterization results illustrated that the modulation efficiency and 3-dB modulation bandwidth are modified as both the gain-to-modulation section lengths and bias current density in each section are varied. The varied carrier density in the two effective sections yields a modulation transfer function modified from the conventional two pole response of uniformly biased semiconductor lasers [2, 13]. Table 1 tabulates the ratio of current densities in both the modulation and gain section with respect to the modulation enhancement achieved.

Table 1. Current Density Ratio vs. Modulation Enhancement in the Gain Lever Effect

Response at 0.4 GHz (dBm)	Response at 1.0 GHz (dBm)	I_{gain} (mA)	J_{gain} (A/cm ²)	I_{mod} (mA)	J_{mod} (A/cm ²)	Modulation Enhancement at 0.4 GHz	Modulation Enhancement at 1.0 GHz	$\frac{Jgc}{Jm}$
-78.8	-73.9	150.00	500.0	10.00	500.0	0.0 dB	0.0 dB	1.0
-66.07	-65.6	151.00	503.3	6.00	300.0	12.8 dB	8.25 dB	1.68
-62.78	-62.9	153.25	510.8	3.50	175.0	16.0 dB	11.0 dB	2.92

The measured resonance frequency of the single-section case ranged from 1.1 GHz to 2.6 GHz as the bias current was increased from 100 mA to 300 mA. The modulation response, $H_R(\omega)$, least-squares-fit (from 0.3-GHz to 2-GHz) with the conventional quadratic response of a single-section semiconductor laser as described by Eq. (1) is given in Fig. 8 [14].

$$|H_R|^2 = \frac{\omega_r^4}{((\omega_r^2 - \omega)^2 + \gamma_{fr}^2 \omega^2)} \quad (1)$$

In Eq. (1), ω_r is the relaxation oscillation frequency, γ_{fr} is the overall damping rate, and ω modulation frequency.

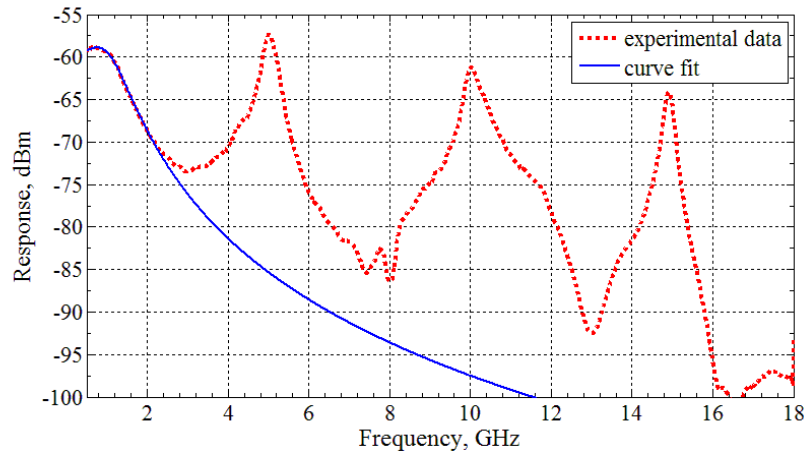


Fig. 8. Single-section modulation response at 100-mA bias current. Prominent resonance peaks are observed at the fundamental and higher order harmonics of the device's free-spectral range. The fit using the conventional response (blue) lacks the enhanced resonance observed experimentally ($\omega_r = 1.15$ GHz, $\gamma_{fr} = 7.53$ GHz)

The long-cavity nature of the device under test yielded a distinctive modulation response due to the order of magnitude proximity of the cavity's free-spectral range (~5 GHz) and its harmonics to the relaxation oscillation frequency. Indeed, the conventional single-section modulation transfer function of a semiconductor laser is well fit by a two-pole low-pass filter response at low frequencies (well below the free-spectral range frequency) but is unable to predict the full experimental response observed in the long-section device when biased as a single-section laser. Clearly the conventional model fails to capture the spatial effects which are important in understanding the modulation of long cavity devices. While such configurations have been addressed in the past [10, 15] they have usually involved lasers with external cavities which is different than the monolithic long-cavity device studied here whose cavity seeks to include only "active" semiconductor sections.

4. Conclusions

The manuscript focused on a novel 8.3-mm multi-section quantum-dot laser. The device allowed gain-to-modulation section contact ratios as high as 15:1, an extreme gain-to-modulation section ratio configuration that has not previously been reported in literature. This allowed the gain-lever effect to be investigated along with a host of other dynamic behavior that came into fruition while gathering experimental data. Compared to the uniform biasing case, a 16-dB enhancement in the modulation efficiency was reported for a case where the small-signal modulated section was biased at threshold and the gain section was biased at an operating point with a high carrier density and hence negligible differential gain. The variation of the modulation section length experimentally illustrated a limit to the effectiveness of increasing to the gain-to-modulation section length ratio and hence an optimal gain-levered operating configuration with respect to section lengths.

The reported results show that by configuring a given laser gain medium into two electrically isolated sections, the control of the direct current operating points of both sections

can result in superior modulation efficiency and modulation bandwidth figures when compared to a single-section, single direct current operating point configuration. The application of this architecture is capable of improving the overall bandwidth capacity of existing semiconductor laser material structures by simply adding a single feature to a device's electrical contact layout.

Another important finding of this work is that the behaviour of multi-section devices, which require each section to be electrically isolated from its neighbour necessitating a small contact separation, suffer from these gaps. This was found by unexpected resonant enhancement obtained when the entire device was uniformly biased. Indeed, this non-uniformity may be sufficient to result in different carrier recovery times along the length of the device which may be sufficient to enable passive mode locking at higher pump currents than those studied in this work. While similar effects have been reported in long-cavity single-section semiconductor lasers it is currently felt that the isolation gaps are responsible for this behaviour in our device and studies to resolve this are in progress.

Acknowledgment

N. Usechak was supported by Dr. Arje Nachman through an Air Force Office of Scientific Research grant (12RY09COR). The views expressed in this article (88ABW-2013-3702) are those of the authors and do not reflect the official policy or position of the United States Air Force, Department of Defense, or the U.S. Government.